

## Grid Connected Single-Phase PV inverter with Novel Control Strategy of Suppressing DC Current Injection to the Grid

**Shaik Tajuddin**

PG Scholar,

Department of EEE

VVIT Engineering College, Nambur, Guntur.

**P. Mahmood Khan**

Assistant Professor,

Department of EEE

VVIT Engineering College, Nambur, Guntur.

### Abstract

*PV inverters without the isolation transformer become more attractive due to higher efficiency and lower weight. However, it may exist DC offset current problem and is critical to the power system. In this paper a novel control strategy of suppressing DC current injection to the grid for PV inverters is investigated. It is based on the idea of accurately sensing the DC offset voltage of PV inverter output. Since DC component of the inverter output can be eliminated, DC injection to the grid can be effectively suppressed. Finally the control scheme is verified by the experiment.*

**Index Terms**—DC current injection, PV inverter, DC offset voltage, DC suppression loop, Grid

### 1. INTRODUCTION

Due to higher efficiency and smaller size, PV inverters without isolation transformers become more attractive in grid-connected photovoltaic systems [1]-[4], [25]-[36]. However, generally they are unable to automatically suppress DC current injection [5], which may cause the saturation of distribution transformers in the grid and result in poor power quality, higher loss, overheating in the power system [1], [6]-[7], [18]. Consequently, standards and regulations have been formulated to limit PV inverter DC injection to the grid [9]-[11].

To suppress DC injection, some control methods have been proposed [1], [6]-[7], [12]-[17], [23]. The methods of DC current injection suppression can be mainly classified into four categories: blocking DC current with the capacitor, novel inverter topology with DC current suppression ability, current-detection control and voltage

detection control. The method of blocking DC current with the capacitor uses a capacitor serially connected between the inverter and the grid [12]. It requires a bulky and expensive capacitor and may cause extra loss. [22] developed a method to block DC current by using virtual capacitor, however, the dynamic response of the closed loop control system was affected by the virtual capacitor.

The method of applying inverter topology with DC current suppression ability uses inherent structure of the inverter topology which can prevent DC current from injecting into the grid, e.g. the half bridge inverter [13]. However, few practical topologies exist. The method of current-detection control uses current sensors to detect the DC current injection to the grid, but its effectiveness is limited by the accuracy of sensor due to the inherent significant zero-drift characteristic of Hall-effect current sensors. To solve the zero-drift problem, an auto-calibrating inverter has been proposed by Armstrong [14]. However, this method requires determining the switch state of the H-bridge in order to measure the inherent zero-drift of the system.

Sharma first introduced a detecting method of DC offset voltage in reference [21]. A small 1:1 voltage transformer and an RC circuit were used to detect the DC offset voltage at the inverter output in the full-bridge grid-connected inverter. And the DC offset in the grid current was eliminated by feeding back the DC offset voltage to the PI controller. Alcock and Bowtell [19] continued studying this method by establishing the mathematical model and verified it. [17] uses a voltage sensor at the inverter output consisting of a differential amplifier and a low pass filter.

DC offset detected at the output of the low pass filter is fed back to the controller. A mathematical model is provided in the paper. However, the experimental results under grid mode were not given. The voltage-detection control method uses sensors to detect the DC voltage offset across the ripple filter [15]. This method implies that very low DC voltage across the filter is measured, which is sensitive to noise. A DC offset detection method is proposed by Giampaolo Buticchi [16]. However, this method needs a nonlinear inductor. Hence, a customized inductor should be designed according to specific systems.

## 2. PHOTO VOLTAIC SYSTEM

A photovoltaic system, also photovoltaic power system, solar PV system, PV system or casually solar array, is a power system designed to supply usable solar power by means of photovoltaics. It consists of an arrangement of several components, including solar panels to absorb and directly convert sunlight into electricity, a solar inverter to change the electrical current from DC to AC, as well as mounting, cabling and other electrical accessories to set-up a working system. It may also use a solar tracking system to improve the system's overall performance or include an integrated battery solution, as prices for storage devices are expected to decline.

Strictly speaking, a solar array only encompasses the ensemble of solar panels, the visible part of the PV system, and does not include all the other hardware, often summarized as balance of system (BOS).

PV systems range from small, roof-top mounted or building-integrated systems with capacities from a few to several tens of kilowatts, to large utility-scale power stations of hundreds of megawatts. Nowadays, most PV systems are connected to the electrical grid, while stand-alone or off-grid systems only account for a small portion of the market. Operating silently and without any moving parts or environmental emissions, PV systems have developed into a mature technology that has been used for fifty years in specialized applications, and grid-connected

systems have been operating for over twenty years. A roof-top system recoups the invested energy for its manufacturing and installation within 0.7 to 2 years and produces about 95 percent of net clean renewable energy over a 30-year service lifetime.

As new installations are growing exponentially, prices for PV systems have rapidly declined in recent years. However, they vary by markets and the system's size. In the United States, prices for utility-scale systems were around \$2.50–\$4.00 per watt in 2012,<sup>[4]</sup> while prices for smaller roof-top systems in the highly penetrated German market fell below €1.40 per watt in 2014.<sup>[5]</sup> In that market, solar panels make up for 40 to 50 percent of the overall cost, leaving the rest to installation labor and to the PV system's remaining components.<sup>[6]</sup> Solar power based on thermal energy, such as concentrated solar power or panels for water heating, are not components of a photovoltaic system.

## 3. NOVEL DC CONTROL STRATEGY

The Full-Bridge PV inverter without output isolation transformer is shown in Fig. 1. From Fig.1, the grid current reference  $i_{ref}$  can be expressed as

$$i_{ref} = I_{ref} \cos \theta \quad (1)$$

where  $I_{ref}$  is the amplitude of grid current command, and  $\theta$  is the phase angle of grid current which is synchronized with grid voltage by Phase Locked Loop (PLL). PV inverter output generally has DC offset voltage component, which results from disparity of power modules, asymmetry of driving pulses, detection error of current etc. Traditionally a transformer is inserted between the PV inverter and the grid. Although the PV inverter output may have DC voltage component, there is no DC current injection to the grid. However, in the case of the PV inverter without isolation transformer, the inverter output DC offset may cause a significant DC current injection to the grid, which may violate the grid connection standards and cannot be neglected [20]. In order to effectively restrain DC current injection to the grid, a control strategy for a single-phase PV inverter without the isolation transformer is shown in Fig. 2 [17],[24].

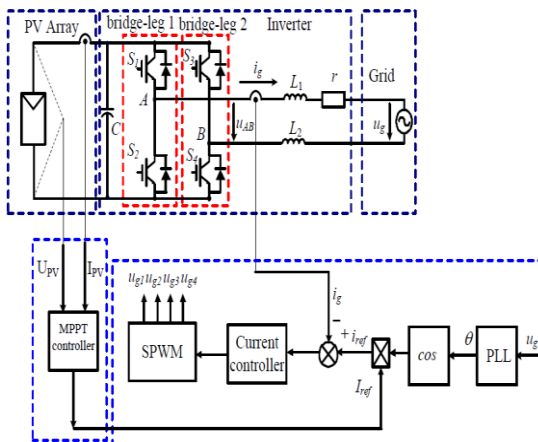


Fig. 1. The original scheme diagram of PV grid-connected inverter

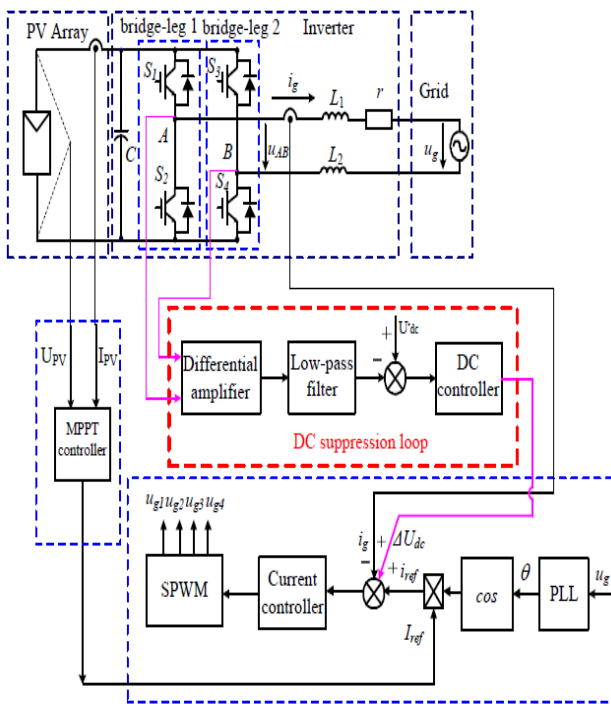


Fig. 2. The novel scheme diagram of PV grid-connected inverter

Compared with Fig.1, an extra DC offset voltage suppression loop is added to the previous control scheme. The DC suppression loop is composed of a differential amplifier, a low pass filter and a DC controller. The input of DC suppression loop is  $u_{AB}$ , which is a high-frequency PWM waveform sampled between the point A of inverter bridge-leg 1 and the

point B of inverter bridge-leg 2. DC offset voltage of  $u_{AB}$  is accurately extracted by a differential amplifier and a low pass filter. Then it is compared with inverter DC voltage reference  $U_{dc\_ref}$  which is set to zero, and DC offset voltage error is obtained. The error is regulated by the integral controller. Finally the output of DC controller  $\Delta U_{dc}$ , which is also the output of DC suppression loop, is added to the grid current reference  $i_{ref}$  of the grid current control loop.

The novel control strategy has two significant features. The first is that the differential amplifier is used to sample the DC offset voltage between the two bridge-leg middle points of Full-Bridge inverter. To accurately detect the DC offset voltage of the inverter switch-side output voltage  $u_{AB}$ , a high-precision differential amplifier with low offset and high CMRR (Common-Mode Rejection Ratio) is needed. The using of differential amplifier can not only reduce the cost, but also avoid the zero-drift by using Hall-effect sensors.

The second one is that DC suppression loop can suppress inverter output disturbances. Therefore the DC current injected to the grid can be effectively suppressed.

#### 4. ANALYSIS OF DISTURBANCE SUPPRESSING EFFECT

The control block diagram of PV grid-connected inverter is shown in Fig.3, which is derived from Fig.1. where  $I_{ref}(z)$  is current reference of the inverter,  $G_c(z)$  is digital controller of current loop, and  $KG$  is the gain from the output of current controller  $G_c(z)$  to inverter switch side voltage, respectively.  $U_{dis}(s)$  represents the disturbance caused by the turn-on and turn-off difference of the four switches, the saturation voltage difference of the four switches, the gate drive signal delay difference of the four switches, and so on.  $L$  is the output filter inductor.  $r$  is the equivalent resistance of output filter inductor  $L$ .  $I_g(s)$  is the grid current of the inverter.  $K1$  is the feedback gain of current loop.  $ADC$  is the analog to digital converter which converts the analog sampling value of  $I_g(s)$  to digital one.  $ZOH$  is zero-order holds which is connected in series between the output of digital controller and  $KG$ .

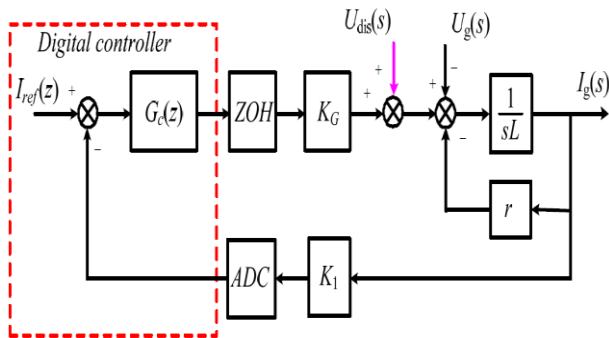


Fig.3. Control diagram for PV grid-connected inverter

From Fig.3, the transfer function in s-domain from disturbance source  $U_{dis}(s)$  to grid current  $I_g(s)$  with the original control scheme can be derived as follows:

$$\frac{I_g(s)}{U_{dis}(s)} = \frac{s \cdot e^{-(T_s \cdot s)}}{s(sL+r) + K_1 K_G (K_{pi}s + K_{ii})} \quad (2)$$

where  $K_{pi}$  and  $K_{ii}$  are the proportional and integral coefficient of current controller, respectively.  $e^{-(s \cdot T_s)}$  is the delay effect considering time delay caused by ADC, digital computation and ZOH, where  $T_s$  is the duration of sampling period [38],  $T_s = 1/f_s$ ,  $f_s$  is switching frequency of PV inverter. In theory, if both the feedback gain of current loop  $K_1$  and ADC are accurate enough, the DC offset of grid current can be eliminated with PI regulator. However, it is actually limited by ADC resolution and accuracy of the current sensor. The maximum grid DC current detecting error  $\Delta I_g$  can be calculated as

$$\Delta I_g = \Delta I_{g1} + \Delta I_{g2} \quad (3)$$

where  $\Delta I_{g1}$  represents error caused by ADC resolution.  $\Delta I_{g2}$  represents error caused by the error of current sensor and conditioning circuit.

#### A. Analysis of Detecting Error Caused by ADC

When N-bit ADC is adopted, the DSP sampled digital value  $I_{gs}$  of the grid current  $I_g$  for the PV grid inverter can be expressed as

$$I_{gs} = I_g \times \frac{2^N}{(1+\beta) \times I_{p-p}} \quad (4)$$

where  $I_{p-p}$  is peak to peak value of the rated grid current, and  $\beta$  represents the overload coefficient of the grid current. From (4), the detecting error of the grid DC current  $\Delta I_{g1}$  caused by the ADC resolution is given by

$$\Delta I_{g1} = \frac{(1+\beta) \times I_{p-p} \times \Delta I_{gs}}{2^N} \quad (5)$$

where  $\Delta I_{gs}$  is ADC error of the DSP.

#### B. Analysis of Detecting Error Caused by Current Sensor and Conditioning Circuit

The grid DC current detecting error  $\Delta I_{g2}$  caused by the error of the current sensor and conditioning circuit is given by

$$\Delta I_{g2} = \frac{\Delta I_{Lem}}{K'_1} + \frac{\Delta I_{Con}}{K'_2} \quad (6)$$

where  $\Delta I_{Lem}$  and  $\Delta I_{Con}$  represent the error caused by current sensor and conditioning circuit, respectively.  $K_1$  is the gain of the current sensor and  $K_2$  is the gain of the conditioning circuit. Therefore, by substituting (5) and (6) into (3), the maximum grid DC current detecting error  $\Delta I_g$  can be calculated as

$$\Delta I_g = \frac{(1+\beta) \times I_{p-p} \times \Delta I_{gs}}{2^N} + \frac{\Delta I_{Lem}}{K'_1} + \frac{\Delta I_{Con}}{K'_2} \quad (7)$$

Let's take a PV grid inverter as an example with parameters listed as follows. Rated power  $P_e = 3$  kW, rated grid voltage  $U_g = 220$  V rms, peak to peak value of the rated grid current  $I_{p-p} = 38.6$  A, overload coefficient of the grid current  $\beta = 0.2$ , the current sensor accuracy  $\Delta I_{Lem} = \pm 0.1$  mA, conversion ratio of the current sensor  $K_1 = 0.0015$ . The conditioning circuit error  $\Delta I_{Con} = \pm 0.2$  mA, the gain of conditioning circuit  $K_2 = 0.25$ . The ADC error  $\Delta I_{gs} = \pm 1.5$  LSB. By substituting the above parameters into (7), the relationship between the ADC bit N and the total grid DC current detecting error  $\Delta I_g$  is drawn in Fig. 4. The solid line shows the relationship between the ADC bit N and the grid DC current detecting error  $\Delta I_g$  with the original control scheme. The dotted line is the DC current limit standard [9]-[11]. It can be seen from Fig. 4 that the grid DC

current detecting error is larger than the standard value with traditional control.

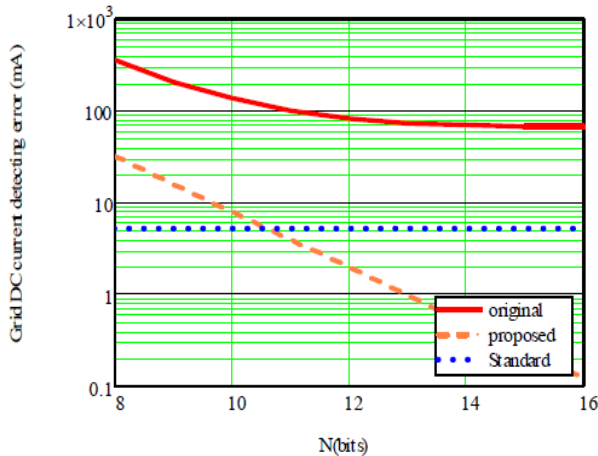


Fig. 4. Relationship between the ADC bits and the grid DC current detecting error, with original control scheme, and with the novel control scheme

C. Analysis of Detecting Error with the Novel Control Strategy

In order to realize that the grid DC current detecting error is less than the standard value, the new control scheme is introduced in this paper. As shown in Fig.5, an extra DC suppressing loop is introduced to the original control scheme of PV grid-connected inverter.  $U_{AB}(s)$  is the voltage between the two bridge-leg middle points of Full- Bridge inverter,  $G_{PI}(z)$  is digital controller of DC suppression loop in z-domain, respectively.  $G_{dc}(s)$  is the feedback gain of DC suppression loop.  $I_{g\_dc}$  is the current of the converter under the new control scheme.

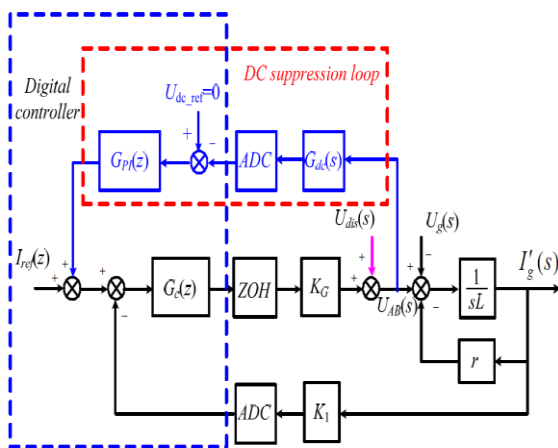


Fig. 5. Control block diagram with novel control scheme

From Fig.5, The relationship between the  $U_{AB}(s)$  and the grid current  $I_g$  is derived as

$$U_{AB}(s) = U_g(s) + (sL + r) \cdot I'_g(s) \tag{8}$$

where  $L$  is filter inductor and  $r$  is equivalent resistance of the filter inductor. For the DC c

$$I'_{g\_dc} = \frac{U_{AB\_DC}}{r} \tag{9}$$

where  $U_{AB\_DC}$  is the DC component of  $U_{AB}(s)$ . The DC suppression loop in Fig.5 is designed to detect the DC component of the converter switch-side output voltage  $U_{AB}(s)$ . The relationship between the DC component of  $U_{AB}(s)$  and the DSP sampling value  $U_{ABs}$  can be derived as

$$U_{ABs} = U_{AB\_DC} \cdot \frac{2^N}{U_{dc\_max}} \tag{10}$$

where  $U_{dc\_max}$  is maximum DC offset voltage. By combining equation (9) and equation (10), we obtain

$$I'_{g\_dc} = \frac{U_{dc\_max} U_{ABs}}{2^N r} \tag{11}$$

Furthermore, the grid DC current detecting error  $\Delta I_{g\_dc}$  with the novel control strategy can be given by

$$\Delta I'_{g\_dc} = \frac{U_{dc\_max} \times \Delta U_{ABs}}{2^N \times r} \tag{12}$$

where  $\Delta U_{ABs}$  is ADC error of the DSP we used. Considering the PV grid inverter system: the value of  $\Delta U_{ABs}$  is  $\pm 1.5LSB$ , maximum DC voltage  $U_{dc\_max}$  is 0.5V,  $r$  is 0.26Ω. The relationship between the ADC bits and the grid DC current detecting error with the novel control scheme is shown in Fig. 4. The solid line is the relationship between the ADC bits and the grid DC current detecting error with the original control scheme. The dash line is the relationship between the ADC bits and the grid DC current detecting error with the novel control scheme. The dotted line represents the DC current limited standard. It can be seen from Fig.4 that the grid DC current detecting error is lower than the standard value with the novel control scheme if the ADC number of bits is greater than 9.



## 6. SIMULATION RESULTS

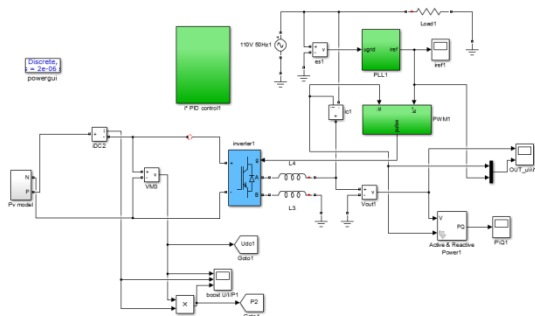


Fig. 8 Simulation Grid Connected Single Phase PV System

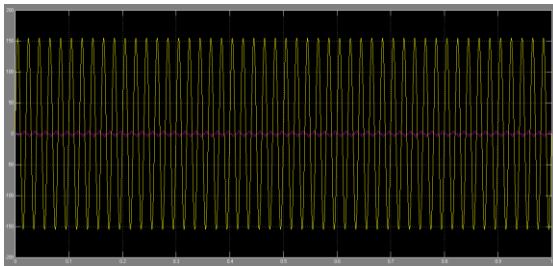


Fig. 9 Grid Voltages and Currents

## 7. CONCLUSION

This paper investigated a novel control strategy to eliminate DC current injection to the grid for single-phase PV inverter without the isolation transformer. It is based on accurately sensing the DC offset voltage between the two bridge-leg middle points of Full-Bridge inverter. The novel control strategy is inherently free from offset measurement errors. Both analysis and experimental results show that the novel control strategy can effectively suppress DC injection current of photovoltaic system under grid-connected condition.

## REFERENCES

[1] R. Gonzalez, E. Gubia, J. Lopez, and L. Marroyo, "Transformerless single-phase multilevel-based photovoltaic inverter", *IEEE Trans. Ind. Electron.*, vol. 55, no. 7, pp. 2694-2702, Jul. 2008.

[2] T. Kerekes, R. Teodorescu, P. Rodriguez, G. Vazquez, and E. Aldabas, "A new high-efficiency single-phase transformerless PV inverter topology,"

*IEEE Trans. Ind. Electron.*, vol. 58, no. 1, pp. 184-191, Jan. 2011.

[3] H. Baeberlin, "Evolution of inverters for grid connected PV Systems from 1989 to 2000," in *Proc. 17th Eur. Photovoltaic Solar Energy Conf.*, Munich, Germany, Oct. 22-26, 2001, pp. 426-430.

[4] J. M. Carrasco, L. G. Franquelo, J. T. Bialasiewicz, E. Galván, R. C. Portillo Guisado, M. A. M Parts, J. I. León, and N. Moreno-Alfonso, "Power-electronic systems for the grid integration of renewable energy sources: A survey," *IEEE Trans. Ind. Electron.*, vol. 53, no. 4, pp. 1002-1016, Jun. 2006.

[5] D. G. Infield, P. Onions, A. D. Simmons, and G. A. Smith, "Power quality from multiple grid-connected single-phase inverters," *IEEE Trans. Power Delivery*, vol. 19, no. 4, pp. 1983-1989, Oct. 2004.

[6] S. B. Kjaer, J. K. Pedersen, and F. Blaabjerg, "A review of singlephase grid-connected inverters for photovoltaic modules," *IEEE Trans. Ind. Appl.*, vol. 41, no. 5, pp. 1292-1306, Sep. 2005.

[7] W. M. Blewitt, D. J. Atkinson, J. Kelly, and R.A. Lakin, "Approach to low-cost prevention of DC injection in transformerless grid connected inverters," *IET Power Electron.*, vol. 3, no. 1, pp. 111-119, Jan. 2010.

[8] V. salas, E. Olías, M. Alonso, F. Chenlo, and A. Barrado, "DC current injection into the network from PV grid inverters," *IEEE Photovoltaic Energy Conversion Conference*, Waikoloa, HI, America, , May. 2006, pp. 2371-2374.

[9] AS 4777.2, Grid connection of energy system via inverters Part 2: inverter requirements Australia. 2002.

[10] IEEE 929-2000, IEEE Recommended Practice for Utility interface of photovoltaic (PV) Systems, 3 April, 2000.

- [11] ER G83/1, "Recommendations for the connection of small-scale embedded generators (up to 16 A per phase) in parallel with public low-voltage distribution networks". Engineering Recommendation, United Kingdom, September 2003.
- [12] R. González, J. López, P. Sanchis, and L. Marroyo, "Transformerless inverter for single-phase photovoltaic systems," *IEEE Trans. Power Electron.*, vol. 22, no. 2, pp. 693-697, Mar. 2007.
- [13] Mohan, Undeland, and Robbins, *Power Electronics: Converters, Applications and design*. New York: Wiley, 2002.
- [14] M. Armstrong, D. J. Atkinson, C. M. Johnson, and T. D. Abeyasekera, "Auto-calibrating DC link current sensing technique for transformerless, grid connected, H-Bridge inverter systems," *IEEE Trans. Power Electron.*, vol. 21, no. 5, pp. 1385-1393, Sep. 2006.
- [15] L. Bowtell and A. Ahfock, "Direct current offset controller for transformerless single-phase photovoltaic grid-connected inverters," *IET Renew. Power Gener.*, vol. 4, no. 5, pp. 428-437, Sep. 2010.
- [16] G. Buticchi, E. Lorenzani, and G. Franceschini, "A DC offset current compensation strategy in transformerless grid-connected power converters," *IEEE Trans. Power Delivery.*, vol. 26, no. 4, pp. 2743-2751, Oct. 2011.
- [17] G. He and D. Xu, "A novel DC loop current control strategy for paralleled UPS inverter system based on decoupled control scheme," in *Proc. Industrial Electronics (ISIE)*, Hangzhou, China, May. 28-31, 2012, pp. 70-75.
- [18] K. Masoud and G. Ledwich, "Grid connection without mains transformers", *J. Electr. Electron. Eng.*, 1999, 19, (1/2), pp. 31-36.
- [19] T. Ahfock and L. Bowtell, "DC offset elimination in a single-phase grid-connected photovoltaic system," *AUPEC*, Melbourne, Australia, Dec. 10-13, 2006.
- [20] Wei Yu, "Key Issues Research on Paralleled UPS Systems," Ph.D. dissertation, Zhejiang University, Hangzhou, Zhejiang, China, 2009.
- [21] R. Sharma, "Removal of DC offset current from transformerless PV inverters connected to utility," presented at the 40th international Universities Power Engineering Conference (UPEC 2005), Cork, Ireland, 2005.
- [22] X. Guo, W. Wu, W. Herong, and G. San, "DC injection control for grid-connected inverters based on virtual capacitor concept," in *Proc. IEEE Electrical Machines and Systems Conf.*, Wuhan, China, Oct. 17-20, 2008, pp. 2327-2330.
- [23] F. Berba, D. Atkinson, and M. Armstrong, "A review of minimisation of output DC current component methods in singlephase grid-connected inverters PV applications," in *Proc. IEEE Environment-Friendly Energies and Applications Conf.*, Newcastle upon Tyne, England, Jun. 25-27, 2012, pp. 296-301.
- [24] G. He, M. Chen, N. Su, R. Xie, and D. Xu, "A novel control strategy to suppress DC current injection of single-phase PV inverter to the grid," in *Proc. IEEE Power Electron. for Distributed Generation Systems Conf.*, Rogers, Arkansas, America, Jul. 8-11, 2013.
- [25] B. Yang, W. Li, Y. Gu, W. Cui, and X. He, "Improved transformerless inverter with common-mode leakage current elimination for a photovoltaic grid-connected power system," *IEEE Tran. Power Electron.*, vol. 27, no. 2, pp. 752-762, Feb. 2012.